NASA SP-5977 (03)
January 1976

TECHNOLOGY UTILIZATION

MANUFACTURING DESIGN AND QUALITY CONTROL

A COMPILATION

NATIONAL AERONAUTICS AND SPACE ADMINISTRATION

Foreword

The National Aeronautics and Space Administration has established a Technology Utilization Program for the dissemination of information on technological developments which have potential utility outside the aerospace community. By encouraging multiple application of the results of its research and development, NASA earns for the public an increased return on the investment in aerospace research and development programs.

Compilations are now published in nine broad subject groups:

SP-5971: Electronics - Components and Circuitry
SP-5972: Electronics Systems
SP-5973: Physical Sciences
SP-5974: Materials
SP-5975: Life Sciences
SP-5976: Mechanics
SP-5977: Machinery
SP-5978: Fabrication Technology
SP-5979: Mathematics and Information Sciences

When the subject matter of a particular Compilation is more narrowly defined, its title describes the subject matter more specifically. Successive Compilations in each broad category above are identified by an issue number in parentheses: e.g., the (03) in SP-5972 (03).

This Compilation is devoted to equipment and techniques that will be of interest in manufacturing and quality control. Section 1 describes testing equipment and quality-control procedures. The second section contains articles that will be helpful in the evaluation, analysis, or selection of materials.

Additional technical information on items in this Compilation can be requested by circling the appropriate number on the Reader Service Card included in this Compilation.

The latest patent information available at the final preparation of this Compilation is presented on page 26. For those innovations on which NASA has decided not to apply for a patent, a Patent Statement is not included. Potential users of items described herein should consult the cognizant organization for updated patent information at that time.

We appreciate comment by readers and welcome hearing about the relevance and utility of the information in this Compilation.

For sale by the National Technical Information Service, Springfield, Virginia 22161

Contents

Section 1. Quality-Control Testing and Procedures

MEASUREMENT OF DIMENSIONS AND ALINEMENT WITH OPTICAL INSTRUMENTS

For several centuries, navigators, surveyors, and builders have used optical instruments as measuring devices. Today, industry is applying similar techniques in measuring alinement and dimensions of finished products. Indeed, it is not uncommon to encounter products that meet the dimensional requirements of one part in 200,000 regardless of size. To meet such requirements, optical inspection tools are used instead of micrometers, calipers, surface plates, or gages, particularly in measurements of large components and systems. This technique, called optical tooling, is already in use in the aerospace industry.

To meet increased demands for personnel training in optical tooling, an advanced manual entitled "Optical Alinement" has been published for use as a handbook in conjunction with an advanced optical alinement training course. The course, as contained in this manual, encompasses the principles involved in determining and applying the proper optical tooling devices to fulfill the precise measuring requirements.

The information covered by the manual incorporates such subjects as versatility of optical alinement, interpretation of design specifications in relation to optical tooling selections, and tooling limitations. Topics include the following:

1. discussion of design tolerances and references,
2. calibration and test of optical tooling instruments,
3. planning of optical alinement,
4. alinement of jaws which hold down rocket boosters during static firing,
5. determination of the geometric thrust vector for rocket engine alinement by establishing the centroid of the throat and exit areas,
6. alinement of rocket power units,
7. determination of flatness of canted planes, and
8. establishing a true north line by observation of Polaris.

Source: W. F. Dendy
Marshall Space Flight Center
(MFS-22168)

Circle 1 on Reader Service Card.

ACCEPTANCE TEST FOR ACCELEROMETERS

Many self-generating accelerometers produce spurious data, or spiking, when used to measure low-level low-frequency vibration in high-level wideband vibration environments. An acceptance test has been developed to reproduce the spurious outputs that are the same as those generated on the test hardware during actual operation, so that these spiking accelerometers can be removed from the available inventory. The test consists of exciting the accelerometer along its transverse axis with high-level wideband vibration. The output is then filtered through an 800-Hz breakpoint low-pass filter, as shown in Figure 1. The vibrator used has a frequency range of from 60 to 10,000 Hz at a rated peak acceleration of 100 g. The first fundamental axial resonant mode of the shaker is approximately 7,000 Hz.

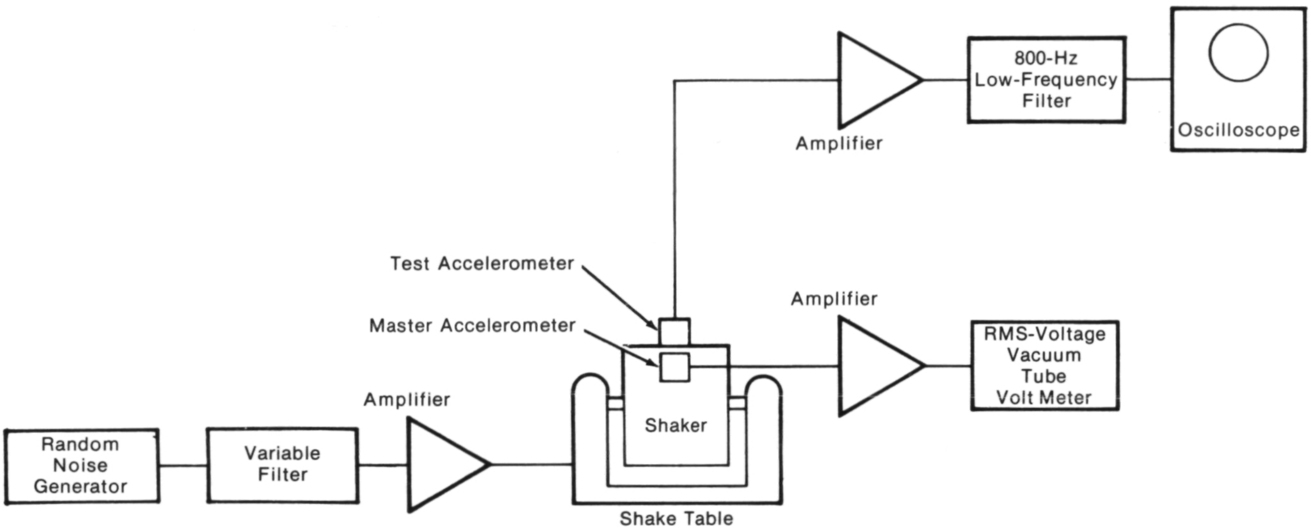

Figure 1. Acceptance Test For Accelerometers

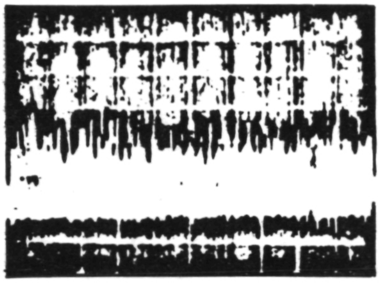

Positive Spiker

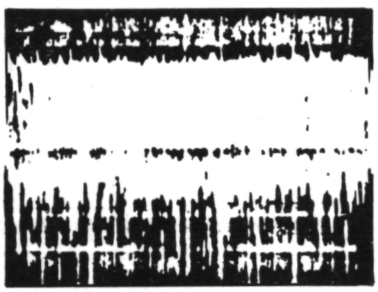

Negative Spiker

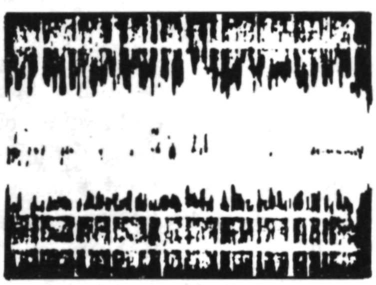

Symmetrical Spiker

Figure 2. Three Types of Spiking

The accelerometer is connected to the input of a unity gain amplifier with an internal low-pass filter with breakpoint set to 10,000 Hz. The output of the amplifier is connected through an 800-Hz breakpoint low-pass filter to the input of a storage oscilloscope. The spiking is produced in the test accelerometer by varying the bandwidth of the random excitation. The bandwidth necessary to produce spiking varies with the accelerometer tested. Figure 2 illustrates the three types of spiking that have been reproduced: positive, negative, and symmetrical. The apparatus needed for conducting these tests can be easily assembled from commercially available equipment at a moderate cost.

Source: G. D. Gullick of
Rockwell International Corp.
under contract to
Marshall Space Flight Center
(MFS-19250)

Circle 2 on Reader Service Card.

FATIGUE TESTING DEVICE

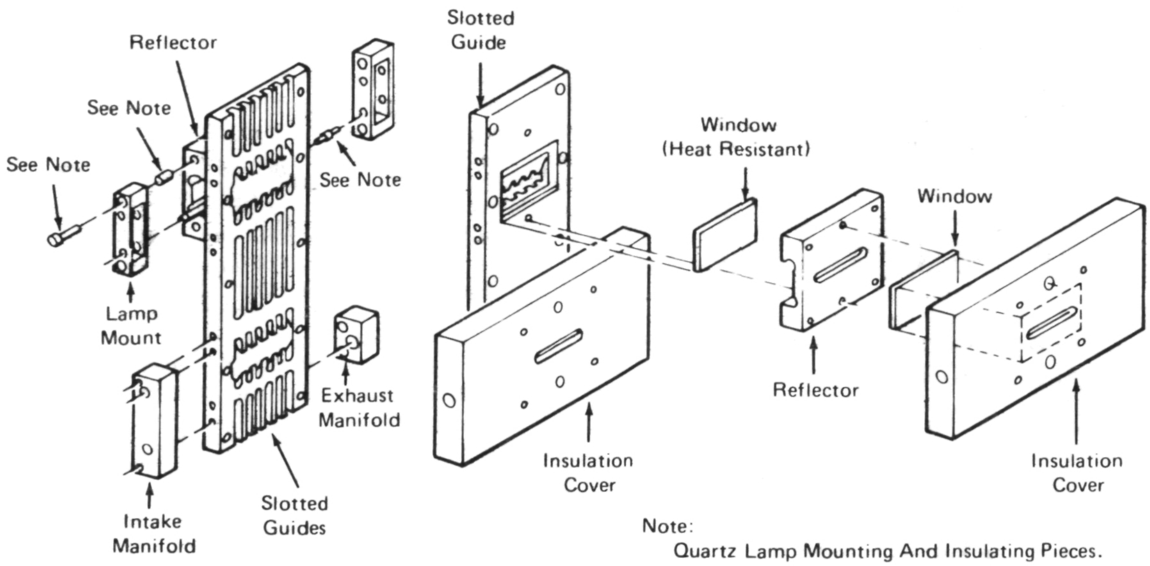

An antibuckling assembly has been developed which prevents buckling of a sheet-metal fatigue specimen when axial compressive load is applied. It has provisions for cyclic heating and cooling of the specimen during testing; it permits simultaneous tests at two locations on the specimen; and it has ports for visual, optical, or photographic monitoring of fatigue crack propagation in the test specimen.

The main components of the assembly (see illustration) are the slotted guides. The slotted guides are used in pairs and are placed over the test specimen with the slotted sides of the guides facing the specimen as it is mounted in the fatigue machine. Shims are inserted between the guides in such a manner that neither the shims nor guides interfere with the test specimen. With the guides in this position they assure that the specimen does not buckle when compressive loads are applied. The guides contain passages for the movement of air to cool the specimen, a mounting for a heat source to heat the specimen, and ports for viewing fatigue cracks.

Reflectors, upon which are mounted quartz-envelope heating lamps, reflect radiant energy to the test specimen through the viewing ports in the guides. The viewing ports in the guides are covered with a heat resistant window which prevents air from circulating and disrupting the temperature uniformity of the specimen.

The test specimen is cooled by pressurized air through one end of the intake manifold and the channels in the guides. A special fitting assures that the air supply to each of the test areas is equal. The heated air is expelled through another port in the intake manifold and through the exhaust manifold.

Similar assemblies may be designed to accommodate specimens with other than two test sections and of different shapes. Cooling at different rates may be achieved by using media other than compressed air. Heating rates are dependent on the type of controller used. In this device temperature may be cycled from room temperature to 588 K (600° F) to room temperature in less than one minute.

Source: F. E. Eichenbrenner and L. A. Imig
Langley Research Center
(LAR-10426)

No further documentation is available.

RELAY-COIL CONNECTION INTEGRITY TEST

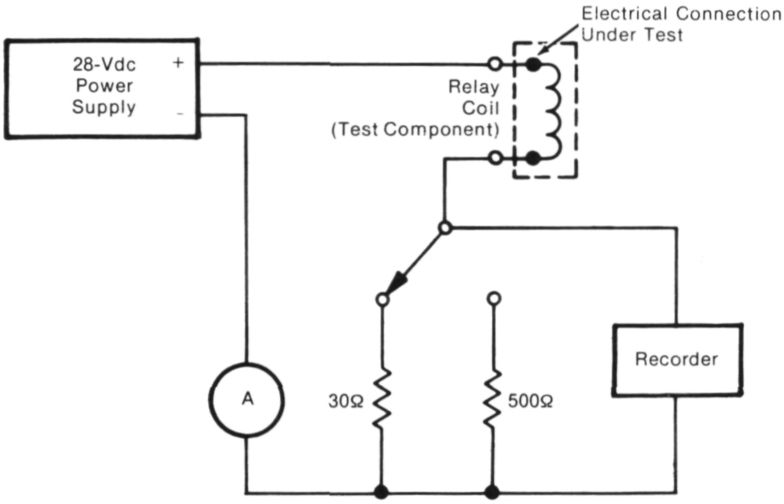

Figure 1. Connection-Integrity Test Apparatus

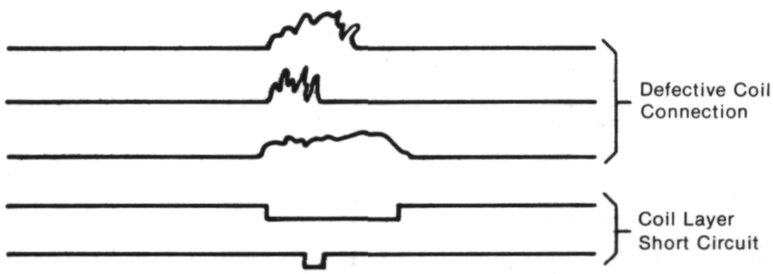

Figure 2. Defective Connection Profiles

A connector integrity test can be used to screen out relays with poor or intermittent coil connections. The test can be applied to completely assembled and potted relays.

The packaged relay is first placed in a temperature chamber. A regulated power supply applies 28 to 32 V (as required) to the coil through a 30-ohm resistor that is connected in series with the coil through a switch (Figure 1). An isolated (floating) recorder is connected across the resistor. The temperature in the chamber then is raised to 150° F (65° C). The coil is allowed to remain at this temperature for 2 to 4 hours and then is deenergized. This procedure drives contaminants which adhere to the coil windings onto the coil connections. A resistor having a value between 1/3 and 1 times that of the coil resistance is then switched into series with the coil, and 2.0 V are applied across the circuit, generating approximately 1 mA in the coil. The chamber temperature is dropped to -65° F (-55° C) and then is returned to room temperature. The current trace is recorded until 15 minutes after room-temperature stabilization. A good coil will produce a linear current trace, while a poor connection will produce intermittent wiggles or sharp deviations from linearity (Figure 2).

This nondestructive method can be used as an acceptance test to screen out potentially defective relays. An available report includes the complete procedure and samples of recordings of the current through defective connections and relay coils.

Source: O. H. Aufdemberg of
Rockwell International Corp.
under contract to
Marshall Space Flight Center
(MFS-24485)

Circle 3 on Reader Service Card.

DYNAMIC TESTING OF COMPLEX STRUCTURES

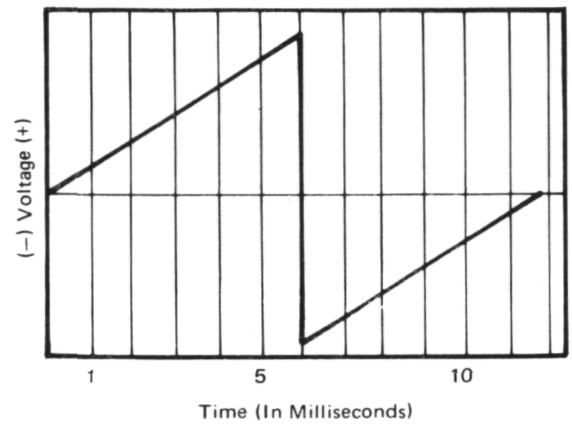

Figure 1. Synthesizer Output

Because it cannot be made by theoretical techniques, the prediction of the dynamic behavior of complex structures, such as automobiles or aircraft, requires special testing methods.

The response of the structure is determined under impulses large enough to create severe strains. An electrodynamic shaker delivers an impulse load as large as 158×10^3 newtons (35,000 pounds force) for a duration as short as 0.8 millisecond. The shaker can provide impulses to nearly any point on the structure and can deliver repeated pulses of varying force and duration with practically no change in the test arrangement.

An electrodynamic shaker is used to deliver the impulse. The shaker has a striker which delivers the impulse by impacting a striker-plate that is placed on the structure to be tested. The striker and striker-plate are both made from cemented tungsten because this impact resistant material has the high modulus of elasticity necessary to achieve a short pulse duration.

Connected between the striker and the shaker is a force transducer consisting of a quartz load link of 158×10^3 newtons capacity held between a base and impact cap.

The motion of the shaker is controlled by an exact waveform synthesizer. The shape of the synthesizer output is shown in Figure 1. The shaker is programed to deliver the impulse at the point of maximum shaker velocity as shown in Figure 2. Because the gap between the striker and the striker-plate is held constant, the pulse amplitudes are varied by changing the duration of the velocity pulse. This adjusts the velocity of the shaker upon impact. An impulse of long duration may be delivered by shaping the velocity of the shaker, as shown in Figure 3, with the striker and striker-plate in contact.

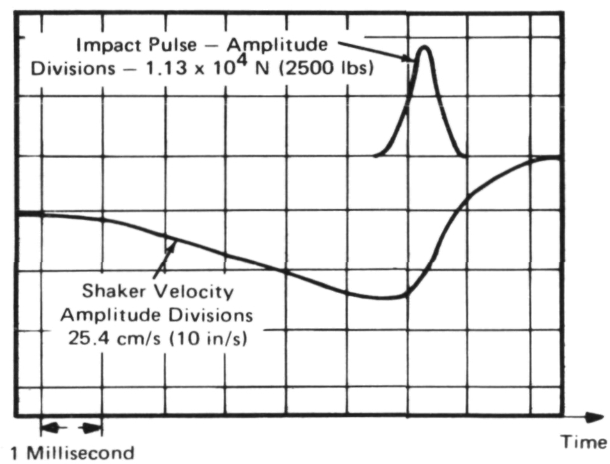

Figure 2. Shaker Velocity

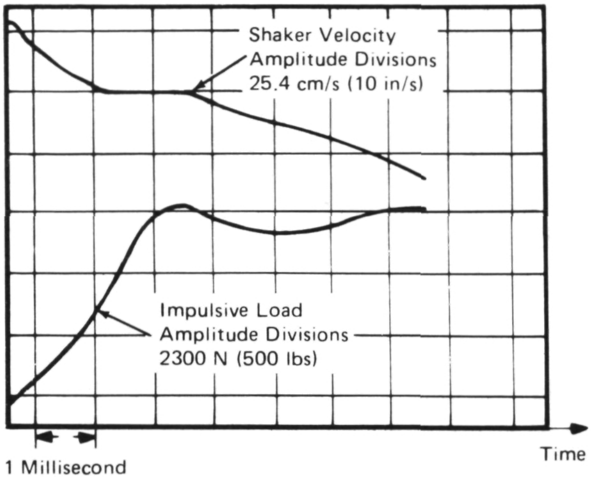

Figure 3. Shaping Velocity of Shaker

Strain gauges placed on the structure are used to measure the effects of the impact. During a typical test, approximately forty specimen-responses are recorded for post-test analysis on a multiplex analog computer.

Source: Charles Birs and Peter Anderson of
Grumman Aerospace Corp.
under contract to
Johnson Space Center
(MSC-12569)

Circle 4 on Reader Service Card.

PROTOTYPE ULTRASONIC INSTRUMENT FOR QUANTITATIVE TESTING

Ultrasonic technology has considerable potential for evaluating small discontinuities in solid materials. For example, many individual operators perform weld evaluations satisfactorily for a particular application; but when several of them evaluate the same specimen, different results are generally obtained. Obviously, uniformly-calibrated ultrasonic instruments are not being used. Furthermore, the basic characteristics of the instruments differ. These facts contribute to the mistrust many people have of ultrasonic technology and consequently many designers do not specify use of the method.

An ultrasonic instrument has been developed for use in quantitative nondestructive evaluation of material defects. The instrument is provided with a standard pulse source and transducer for each frequency range selected and includes integral aids that allow calibration to prescribed standards.

The instrument consists of a special pulser/receiver that plugs into a standard oscilloscope, a special rf power amplifier, a standard decade oscillator, and a set of broadband transducers for typical use at 1, 2, 5, and 10 MHz. In addition, the system provides for its own calibration and presents a quantitative indication of time-base and sensitivity scale factors and some measurement data on the oscilloscope. Performance includes a velocimetry capability of better than 0.1 percent.

The general features of the system include the specified integral aids to calibration of a high-gain broadband receiver, a means of adjusting the receiver gain in discrete steps, and mechanical vernier adjustments to calibrate the steps in receiver gain. A standard high frequency source is used to generate pulses of known width and amplitude with a means of adjusting the transmitted pulse width and pulse repetition rate in steps of known magnitude. Other features include mechanical vernier adjustments to calibrate pulse characteristics, methods of adjusting the output voltage of the transmitter continuously over a specified range, and provision for a voltage indicator for transmitter output.

Source: L. C. Lynworth, J. L. Dubois, and
P. R. Kranz of
Panametrics, Inc.
under contract to
Marshall Space Flight Center
(MFS-22350)

Circle 5 on Reader Service Card.

IMPROVEMENT OF SCREENING METHODS FOR SILICON PLANAR SEMICONDUCTOR DEVICES

Silicon planar semiconductor devices are characterized by highly time-dependent failure mechanisms that are not effectively removed by conventional high-reliability screening techniques. A more sensitive method of selecting these devices has been developed for long-life applications. The method is applicable to integrated circuits at the highest level of integration as well as to discrete diodes and transistors.

Sensitive test-pattern chips are interdispersed on the same wafers as functional MOS or bipolar integrated circuits. These are used to detect and screen, in a relatively short period of time, highly time-dependent failure mechanisms. Results indicate that failure mechanisms are not necessarily the same for all wafers from a given diffusion lot, and that ultrahigh reliability selections must be based on a wafer-by-wafer evaluation. Both visual and electrical correlations have been observed between the measurements made on the functional and on the test-pattern structures, and these can be economically applied as standard screening techniques.

The test-pattern structures help set rejection criteria better than those based entirely on functional integrated-circuit-device performance. To ensure overall reliability, the test-pattern screen techniques should supplement but not replace electrical, visual, and thermal screening of the functional devices themselves.

MOS and bipolar technologies have different failure mechanisms; these are due primarily to their different electrical characteristics and physical mechanisms. The failures peculiar to each construction technique and the failures common to both techniques have been studied and are discussed in an available report.

Source: W. M. Berger of
Philco-Ford Corp.
under contract to
Marshall Space Flight Center
(MFS-22928)

Circle 6 on Reader Service Card.

PROBABILITY OF SURVIVAL

A computer program has been developed to implement a mathematical technique for determining the probability that a piece of equipment will perform in the manner specified and for the period of time required by its design specifications.

The program generates punched-cards which may be used to plot time versus the probability of survival. The conclusions obtained from the results of the program will be meaningful only if the reporting system for component failures is regular and accurate. The program consists of approximately 200 punched-cards and is written in FORTRAN IV for the IBM 1620 computer.

Source: Caltech/JPL
under contract to
NASA Pasadena Office
(NPO-11182)

Circle 7 on Reader Service Card.

OPERATIONAL READINESS EVALUATION METHOD

An operations readiness evaluation (ORE) method employs system engineering techniques, coupled with equipment-reliability and maintainability properties, to predict the probability of accomplishing a task at a specific date. Equipment failure rates, restoration times, and operational timelines are the basic inputs for the method. The input data are treated analytically using probability methods, and the results are expressed in success/failure probabilities. The method can be used in problem identification, trade-offs, operations scheduling and resource allocation. Previous methods have utilized independent reliability and maintainability evaluations, but the key feature of the ORE method is the consolidation of reliability, maintainability, and system engineering, thus making trade-offs and optimization possible.

The major steps of the ORE procedure are: (a) generation of an operations schedule identifying equipment used and their usage timelines. (b) determination of the failure rates for the equipment involved, (c) determination of repair time for items most likely to fail and the number of spares required to support maintenance activities, and (d) consolidation of the data and performance of the probability analysis.

Source: R. F. Wadsworth and G. S. Yamashita of
Rockwell International Corp.
under contract to
Johnson Space Center
(MSC-17395)

Circle 8 on Reader Service Card.

A FREQUENCY RESPONSE METHOD FOR THE ANALYSIS AND DESIGN OF MULTIRATE SAMPLED-DATA SYSTEMS

A frequency response design technique has been devised for single-input/single-output, multirate sampled-data systems. Such systems are needed if a digital controller is to provide output information at a rate different from the basic system sampling rate. The technique is applicable to linear systems having a sampling operation that can be represented by an impulse modulator followed by a zero-order hold. Also, the fast-rate sampling frequency must be an integer multiple of the slow-rate sampling frequency. The technique utilizes a bilinear transformation, which enables one to employ a Bode plot design procedure. An upper bound for the selection of the ratio of sampling frequencies, n, has also been developed.

In conjunction with the development of the frequency response design technique, the digital computation of the multirate-system frequency response is discussed. The infinite series form of the s-domain multirate-system transfer function is developed for this purpose. Finally, a multirate-system identity is presented to assist in determining the z_n-form of the multirate-system transfer function. This identity then is utilized to determine the multirate-system output for a quantization disturbance at the digital controller output accumulator.

Source: C. L. Phillips of
Auburn University
under contract to
Marshall Space Flight Center
(MFS-22051)

Circle 9 on Reader Service Card.

A REPORT ON THE INTERFACE PRINCIPLE

The interface principle is a methodology for the development of long-life mechanical and electromechanical components. It subscribes to the "weak-link concept", i.e., the simple premise that the operational longevity of a mechanical or electromechanical component, as a whole, is directly related to the longevity of its weakest operational interface between moving parts. Accordingly, the study of a component at the operational or dynamic interface level is the basic working mechanism in the application of this principle. An operational or dynamic interface is defined as the most elementary combination of mechanical elements in a component providing surfaces in contact and under relative motion.

In order to fully exploit the merits of the interface principle, it must be applied to overall component development in its most preliminary phases, preferably during design. In support of component design, interface design concepts, based on wear analysis of numerous existing components, have been tabulated into fifteen categories. In each interface category, the interfaces are tabulated in order of increasing wear rating (increasing assessed-wear capability). To date, these tabulations include over 240 interfaces, representing approximately 150 different concepts. It is primarily within the area of weak-link identification that the tabulations, including their wear ratings and assessments, are most valuable. They will assist in the design of components and in the selection of design concepts.

The report also discusses the application of the interface principle in wear analysis. The experience with nonmetallic materials, described in the report, can be applied to many design problems. Included are tabulations of materials, properties, recommended applications, life times, and other experimental data.

Source: E. D. Storms and D. K. Huzel of
Rockwell International Corp.
under contract to
Marshall Space Flight Center
(MFS-24479)

Circle 10 on Reader Service Card.

UNIFORM RANDOM-NUMBER GENERATORS

The need for sequences of numbers that appear to be drawn from particular probability distributions has become increasingly more important with the wide use of simulation and Monte Carlo methods. The purpose of a new report is to present automated procedures for the production of these pseudo-random numbers consistent with the above criteria. In automating the random-number generators, the emphasis is placed upon the uniform distribution. The production of such sequences of numbers, or so-called "pseudo-random" numbers, must be simple, fast, accurate, and, most importantly, reproducible.

Most random-number generator subprograms found in computer libraries are coded in complex machine language and therefore tend to increase, rather than to alleviate, the existing confusion concerning the generation of random variables. FORTRAN subprograms have been developed for the generation of uniform pseudo-random numbers on the unit interval (0, 1). These generators are of the mixed-multiplicative congruential type, and the method is that of Marsaglia and Bray. The subprograms described are for the Univac 1108, the CDC 3200, and the SDS 930 digital computers. A method for generating normal random variables from uniform variables is also included.

Source: W. R. Farr
Marshall Space Flight Center
(MFS-21990)

Circle 11 on Reader Service Card.

HAZARD REDUCTION THROUGH APPLICATION OF ALLIED EXPERIENCE

A report presents a systematic approach for the progressive application of retained safety-related experiences and a method by which program safety performance can be assessed. Most importantly, a method is given for determining the effectiveness of the application of retained safety experiences. The technique can be used effectively by both aerospace and nonaerospace industries.

A series of special criteria are established for design, manufacturing, test, and operations, including handling, transportation, servicing, and maintenance. The technique includes participation by those people directly responsible for and most knowledgeable of the hardware. It provides a simplified method for hazard identification, which can be used independently or in support of more sophisticated hazard-analysis techniques. The engineering, quality, reliability, and testing disciplines are all effectively coordinated to achieve improved safety. The system can be implemented on any program, subsystem, or equipment item of any size or complexity, and it will provide management with effective reports of results to aid in making decisions associated with cost, schedule, and risk.

Source: E. M. McNail of
Martin Marietta Corp.
under contract to
Marshall Space Flight Center
(MFS-22855)

Circle 12 on Reader Service Card.

Section 2.
Design and Material-Selection Techniques

STATISTICAL ENERGY ANALYSIS TECHNIQUES

Classical modal analysis techniques for predicting dynamic response work well in the frequency range of the lower structural resonances. However, when these techniques are extended into the higher frequency range, the complexity and size of the model and the required solution time increase rapidly. Consequently, classical solutions in the high-frequency range are well beyond the current state of the art for computer hardware. Statistical energy analysis (SEA) techniques can successfully circumvent these problems, which arise when high-frequency random-vibration environments are studied in order to predict the dynamic response of large aerospace vehicles.

A report documents the results of a study, using experimental data from complex vehicular structure tests, to evaluate the use of SEA with general structural systems. The report shows the development of the basic SEA equations. These expressions are then expanded to cover complex structures and are put into a form readily compatible with available matrix abstraction programs. An analytical study of elementary systems is performed yielding some useful information concerning SEA and high-frequency response in general. The major portion of the report is devoted to the evaluation of SEA in application to a complex structure: an elliptical cone excited with a range of acoustic configurations. In many respects, this represents a more complex analysis problem than that for typical vehicles. Considering the complexity of this structure, together with the various types of acoustic input configurations, one can expect the results to be valid for a wide range of structural problems.

This application incorporates a test program that successfully provided damping and coupling parameter values through the use of very simple test methods. A technique for introducing acoustic energy into the SEA model is derived and gives good results with reverberant acoustic fields. This statistical structural analysis, in conjunction with the simple test methods, resulted in high-frequency vibration-response predictions having an accuracy of ±3 dB in comparison with test measurements. Frequency scaling methods are presented that may be used to evaluate the frequency range in which this accuracy can be expected for general structures.

Source: R. F. Davis and D. E. Hines of
McDonnell Douglas Corp.
under contract to
Marshall Space Flight Center
(MFS-22780)

Circle 13 on Reader Service Card.

FRACTURE-MECHANICS EQUATIONS FOR CYCLIC CRACK GROWTH

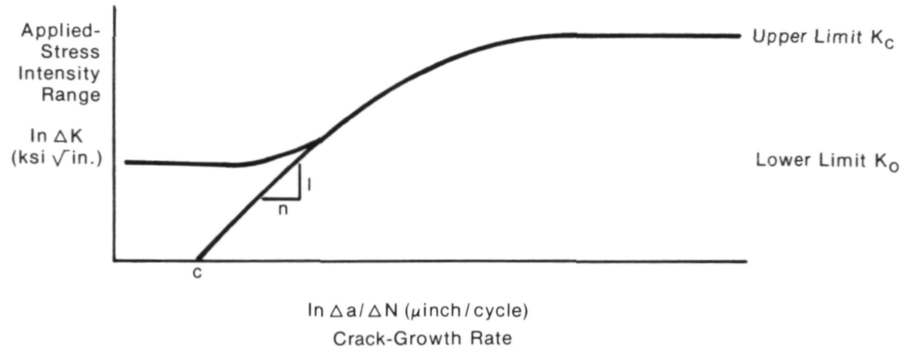

$$\frac{\Delta a}{\Delta N} = \text{Exp}\left[\frac{n\cdot(\ln K_c - \ln K_0)}{2}\,\text{arctanh}\left\{\frac{\ln\Delta K - \frac{\ln[K_c(1-R)] + \ln K_0}{2}}{\frac{\ln[K_c(1-R)] - \ln K_0}{2}}\right\} + \ln\left\{C\,\text{Exp}\,\frac{(\ln K_c + \ln K_0)\,n}{2}\right\}\right]$$

Applied Stress vs. Crack Growth

A generalized expression has been developed to represent cyclic crack-growth rates as a function of applied-stress intensity. The function is a hyperbolic tangent expression derived from the Paris equation for crack growth. The expression provides rational upper and lower limits on the applied-stress intensity excursion when the crack-growth rates approach infinity and zero, respectively. Four material-dependent constants are incorporated into the expression. Load-ratio effects are described for many materials.

The figure shows the calculated relationship between applied stress and the rate of crack growth. The generalized expression is shown in the figure, where:

$\frac{\Delta a}{\Delta N}$ = the crack-growth rate in micrometers/cycle,

and the following constants depend on properties of the materials:

- n = the Paris equation exponent,
- K_c = the stress intensity for fracture,
- K_0 = the threshold (lower limit) stress intensity, and
- C = Paris equation coefficient,

and the following are the test input variables:

- ΔK = the cyclic range of the applied-stress intensity
- R = the load ratio

Further available information includes the derivation of the formulas, graphs which compare formula results with previous studies of crack growth, and charts of crack-growth rate versus applied-stress intensity for a number of materials.

Source: J. E. Collipriest, R. M. Ehret, and C. Thatcher of Rockwell International Corp. under contract to Marshall Space Flight Center (MFS-24447)

Circle 14 on Reader Service Card.

ANALYSIS OF RIGIDIZED FIBROUS MATERIALS

Analytical models have been developed to predict the thermal and mechanical properties of rigidized fibrous materials. These materials are being used as high-temperature insulations in situations where the insulation must carry a structural load or is exposed to a flowing airstream. Because these materials are new and there is limited empirical experience for designers, the development of an analytical model to predict structural properties is particularly important.

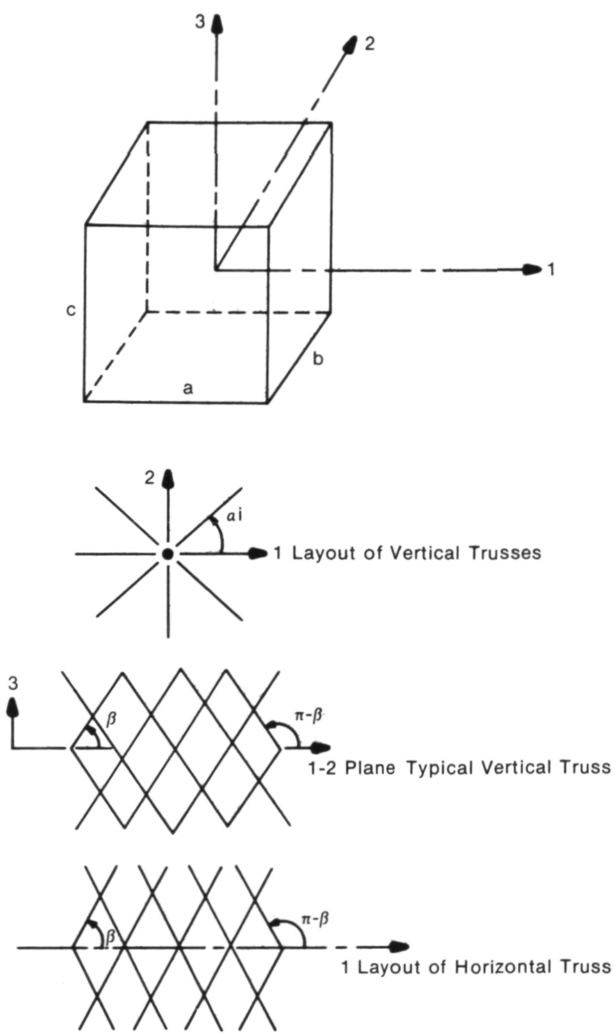

A Typical Space Model

On a microscopic level the low-density fibrous materials are represented as a space frame. The fibers are oriented in three-dimensional space, with bonds wherever fibers touch. Stresses in individual fibers are treated as the combined effect of axial loads, bending stresses due to joint fixedness, and bending stresses due to the initial curvature of the fibers.

The model utilizes a series of different, regular arrays of trusses, having various orientations, to represent the random three-dimensional fiber array. A concept of parallel trusses is used to represent geometric factors such as orientation, fiber-aspect ratio, eccentricity, and volume fraction. Assemblies of trusses are oriented parallel to one of five different planes. A given plane can have any number of trusses (see figure), the interaction of which arises from the constraint that all must have the same average strains. The continuous statistical distribution function defining the fiber geometry is represented by a series of elements having discrete values of each variable.

The combined stress is calculated with the following assumptions:

a. All trusses lying in a given plane have the same average stresses.
b. The fibers in a single truss have the same lengths, diameters, eccentricities, and inclinations.

In this model, failure of the material is defined as a critical accumulation of internal fractures caused by fiber breaks in any plane. A statistical approach is used; as the loading factor is increased in a single plane, fibers in a particular truss break. A redistribution of the load among unfractured trusses results. This may lead to further noncritical fractures or a stable distribution. If the distribution is stable, a greater load is applied until a load sufficient to cause an unstable state, and thus critical failure, occurs.

The following documentation may be obtained at cost from:

National Technical Information Service
Springfield, Virginia 22151

Reference: NASA-CR-2371 (N74-16594), Analytical Study of Rigidized Fibrous Materials

Source: Debal Bagchi, John J. Kibler, and B. Walter Rosen of Materials Science Corp. under contract to Langley Research Center (LAR-11501)

PREDICTION OF TWIN-SPOOL TURBOPUMP OPERATING CHARACTERISTICS

A computer program has been developed to predict the steady-state and transient operating characteristics of a twin-spool turbopump over a wide range of operating conditions. The performance characteristics of the individual turbine and pump components are used as input to the program. The validity of the analytical model used has been demonstrated by comparing predictions with experimental data obtained from tests of completed turbopumps.

The output of the program includes speed, power, pressure, temperature, and normalized performance parameters. A transient solution for flow conditions in the inducer suction line (based on water-hammer theory) has been included in the program as an option for transient cases. Two basic program options allow the input of either a time-dependent main-shaft speed or main-turbine inlet pressure. The program incorporates subroutines for hydrogen fluid properties; these may be replaced with subroutines for other types of fluids.

The approach used in the development of the computer model incorporates the overall characteristic curves depicting the performance of each turbopump component. The analysis is based on several major assumptions:

a. The main-turbine mass-flow rate equals the inducer-turbine mass-flow rate.
b. The flow in the inducer and pump components is incompressible (this does not exclude the computation of density at each station of the pump system).
c. The flow in all components is single phase.
d. The data on component performance characteristics under steady-state conditions can be used to adequately represent the system in a quasi-steady-state solution.
e. For transient solutions, steady-state conditions exist initially.
f. Bearing friction is negligible.
g. The flow in the turbine exhaust system is incompressible.

The program is written in FORTRAN IV, to operate on IBM system/360 computers.

Source: K. G. Kirk of Aerojet-General Corp. under contract to Lewis Research Center (LEW-11079)

Circle 15 on Reader Service Card.

ARBITRARILY-SHAPED DUAL-REFLECTOR ANTENNAS

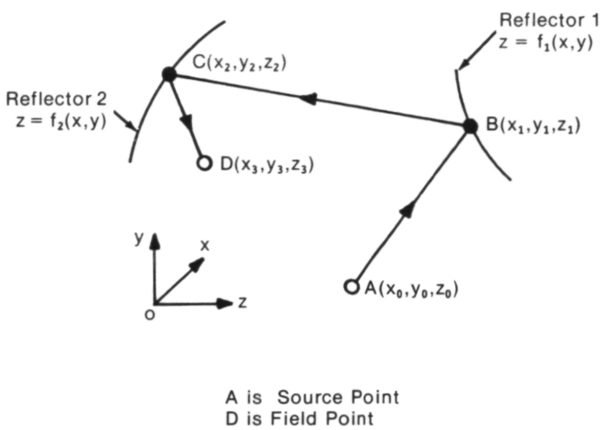

Dual-Reflector Antenna Geometry

One successful type of dual-reflector antenna has the shape of a surface of revolution about an axis on which the feed horn is located. A pair of first-order nonlinear differential equations, derived according to the laws of geometrical optics, are solved to obtain the shapes of the dual reflectors for a given phase and amplitude distribution in the aperture of the second reflector. Although this technique may be extended, in principle, to treat the case in which the feed horn is located away from the axis of the reflectors, the resultant equations are a set of nonlinear partial differential equations which are very difficult (if not impossible) to solve.

In an attempt to circumvent this difficulty the following problem has been analyzed: Assuming that the shapes of the two reflector surfaces are given, find the field distribution in the aperture of the second reflector. To obtain the desired aperture field distribution an iterative trial-and-error method is used to find the final shapes of the dual reflectors. For the initial trial the shapes of the reflectors are assumed to be those obtained according to the previous method for a symmetrical, on-axis feed, dual-reflector system.

A point source is assumed to be located at point $A(x_0,y_0,z_0)$. A ray originating from the point source at A is assumed to be reflected at the point $B(x_1,y_1,z_1)$ on a doubly-curved reflecting surface called surface 1. The reflected ray from surface 1 is again reflected at the point $C(x_2,y_2,z_2)$ on another doubly-curved reflecting surface called surface 2. This reflected ray from surface 2 finally arrives at the field point $D(x_3,y_3,z_3)$. The geometry of this problem is given in the figure. It is assumed that surface 1 may be described by the equation $z = f_1(x,y)$, and surface 2 by $z = f_2(x,y)$.

The analysis assumes that at each point on the reflector, the incident ray is reflected by the tangent plane according to the laws of reflection. The intensity of the reflected wave in a given direction is obtained by applying the principle of the conservation of energy to the total power contained in an incident cone of rays and the total power contained in the associated reflected pencil of rays. The use of the laws of reflection assumes that (1) reflectors 1 and 2 can be regarded locally as plane surfaces, and (2) that the incident wavefront can be regarded locally as a plane wave. In other words the radii of curvature of reflectors 1 and 2, and of the incident wavefront, must be large compared with the wavelength. Condition (2) may be assured by the fact that the reflectors are in the far-zone field of the source.

The phase distribution across the aperture of reflecting surface 2 will depend then on the path length and the phase change upon reflection. The phase length is easily calculated if the point of reflection on the surface is known and if the point of reflection is uniquely defined by Snell's law, which states that the angle of incidence is equal to the angle of reflection.

The achievement of maximum gain requires uniform phase and amplitude distribution across the aperture. Thus it is desirable to design the reflector surfaces so that the requirements on phase and amplitude may be met. A formula has been derived which enables the aperture field distribution to be calculated when the source function and the reflector surfaces are given. A design technique based on the derived formulas has also been developed.

Source: Cavour Yeh of
Caltech/JPL
under contract to
NASA Pasadena Office
(NPO-11883)

Circle 16 on Reader Service Card.

DYNAMIC ANALYSIS OF LARGE STRUCTURES

The experience at the Jet Propulsion Laboratories in the dynamic analysis of large structures is discussed in two reports. The methods described are suited to the analysis of complex three-dimensional structures with plate and beam elements, discrete dampers, and nonlinear elements. Since, in many cases, schedules have not permitted redesign, the analysis procedure is intended to provide final design criteria. Considerable test data are used, and the required computer size and running time are kept to a minimum.

The system to be analyzed is divided into substructures with characteristics represented by displacement functions. The use of displacement functions can reduce the problem of a structure with 7000 degrees of freedom to one of 100 degrees of freedom, with little loss in accuracy if only the lower eigenvalues are significant. Another advantage of the substructure method is that previous analyses of substructures can be utilized in the design of new larger complex structures. The substructure solutions are combined using compatibility relationships, and then the eigenvalues for the entire system are found.

In one example discussed in the report, classical mode analysis is transformed into a frequency domain problem using fast Fourier transforms. The result is a concept of dynamic mass for a complex structure, which appears as an expression analogous to Newton's Law. This combination of the component-mode approach and the frequency domain approach, along with analog simulation, has been shown to be a valuable tool in the analysis of complex structures.

Source: Robert M. Bamford, James R. Chisholm,
John A. Garba, Marc R. Trubert, and
Ben K. Wada of
Caltech/JPL
under contract to
NASA Pasadena Office
(NPO-11903 and NPO-11904)

Circle 17 on Reader Service Card.

THE INFLUENCE OF STRESS RATIO ON FATIGUE-CRACK GROWTH

In structural design and when selecting materials according to fatigue properties, fatigue-crack growth data may be required over a wide range of growth rates and at various stress ratios, R. A systematic procedure has been developed for finding fatigue-crack growth data over a wide range of stress ratios. This procedure is based on a considerable amount of background information on the effects of load interactions on delay, and allows materials to be screened rapidly, using only a limited number of test specimens. It is based on the following three experimental observations:

1. There is no delay in fatigue-crack growth if the maximum load, P_{max} is maintained constant, while the range of cyclic load, ΔP is changed.
2. The period of non-steady-state crack growth is minimized if changes in P_{max} are kept as small as practicable.
3. Thermal equilibrium at the crack tip is not seriously disturbed by small changes in P_{max}, or is reestablished rapidly, following the change in P_{max}.

The test procedure consists of precracking and data acquisition sequences. These sequences are illustrated in Figure 1. The precracking sequence (white bars) is carried out at appropriately high load levels with R equal to 0 or 0.05. After crack initiation (first white bar), P_{max} is reduced in increments approximately 10 percent of the preceding P_{max} (while maintaining R constant) until the desired P_{max} (e.g., 5 kips in Figure 1) is reached. Changes in the load are made only after load interaction effects have been overcome, as indicated by the crack measuring system. Once precracking is completed, P_{max} is increased to start the data acquisition sequence (stippled bars). Enough minimum-load values are used for each P_{max} to cover

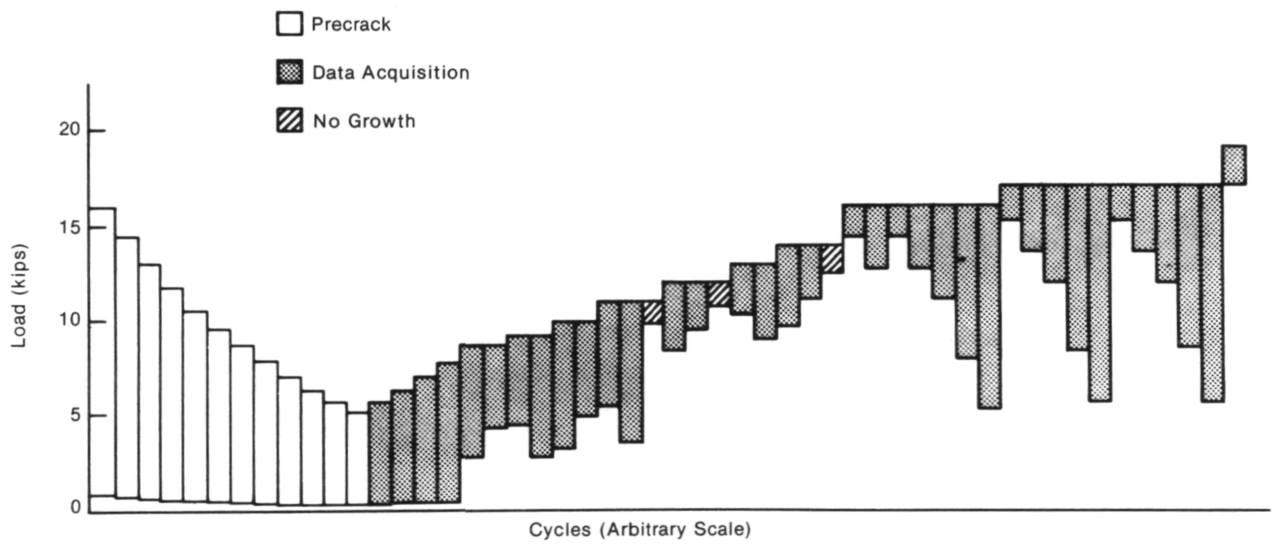

Figure 1. A Typical Load Sequence for the Suggested Test Procedure

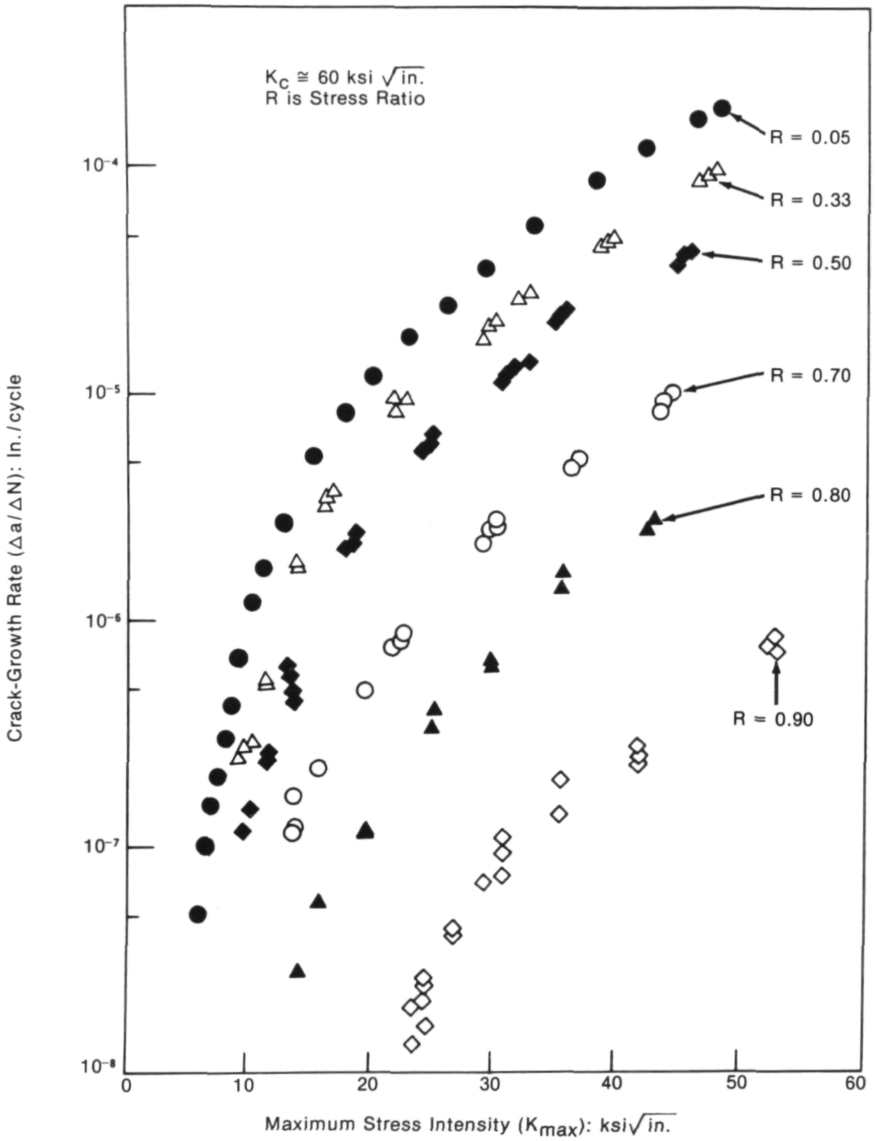

Figure 2. Kinetics of Fatigue-Crack Growth For a Mill Annealed Ti-6Al-4V Alloy Sheet Tested in Air at Room Temperature.

the range of stress ratios of interest. Crack-growth data obtained by this procedure are shown in Figure 2 along with previously obtained data at R = 0.05. Data for R = 0.33 to 0.9 were obtained principally from two 3-inch-wide specimens. The large quantity of data generated using these specimens illustrates the potential economic advantages of this test procedure. Note: Corrosion fatigue-crack growth may involve different crack-growth phenomena which would not be accurately characterized by this procedure.

Source: J. H. FitzGerald and R. P. Wei of Lehigh University under contract to Langley Research Center (LAR-11488)

Circle 18 on Reader Service Card.

PREDICTING BENDING MOMENTS IN MULTI-PLY METAL-BELLOWS FLEX-JOINT ASSEMBLIES

A FORTRAN program has been written which employs empirically and analytically derived equations to predict the bending moment of pressurized bellows-joint assemblies of various designs. Conventional analytical methods are inadequate to predict the maximum bending moments accurately. The data from nine bellows designs at 13 different operating conditions have been analyzed to establish the computer model.

The total pressurized moment is considered to comprise four basic components as follows: (1) the unpressurized-spring-rate (or bending) moment, (2) the bellows-straightening moment, (3) the friction moment, and (4) an empirical correction term. The unpressurized angular spring constant (K) does not depend on angular deflection Θ, unless significant yielding or mechanical binding occurs. Because manufacturers' specifications normally include a tolerance in K of ±20 percent, the maximum moment (K_{max} Θ_{max}) is taken as 1.2 times the nominal moment.

When the bellows are bent under pressure, there is a small lever arm ε, which increases with angular deflection. The distance ε is the length between the bellows axis and the restraining-hinge axis. This particular choice for ε gives the maximum value possible. The moment term is then the product PAε, where P is the internal pressure and A is the mean area of the bellows.

The correction term used accounts for real effects not included in the model. This term has been correlated with the unpressurized-spring-rate moment, the bellows critical-buckling-pressure ratio, and the bellows stress.

The friction can contain up to three components: (1) an internal-ply friction moment, (2) a hinge friction moment, and (3) a stabilizer moment. The ply friction moment is the inter-ply rubbing effect between multi-ply bellows under pressure. The hinge friction moment is the friction force times the lever arm, where the lever arm is the hinge-pin or ball radius. The friction force in this case is the normal load of the pin (or ball) times the coefficient of friction. The stabilizer moment applies only to joint assemblies that have two bellows in series and incorporate an internal stabilizer sleeve. The stabilizer moment contains both a reaction moment and a friction moment, but both are included as friction terms to make the model match test data more closely.

It is primarily the addition of the friction terms that makes this method more powerful in predicting total bending moments. Previous methods ignored the complex effects of inter-ply friction and stabilizer effects. Here these parameters are determined empirically, to substantially improve the accuracy of the calculation.

Source: L. N. Jew of
Rockwell International Corp.
under contract to
Marshall Space Flight Center
(MFS-19226)

Circle 19 on Reader Service Card.

FILAMENT WINDING TECHNIQUE PRODUCES STRONG LIGHTWEIGHT OXYGEN TANKS

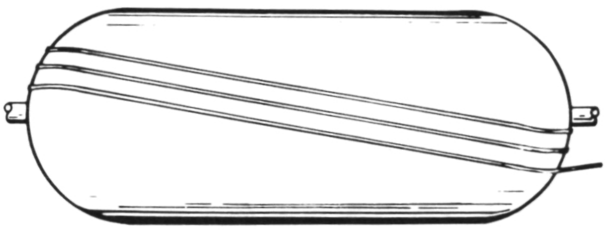

Geodesic Winding Pattern

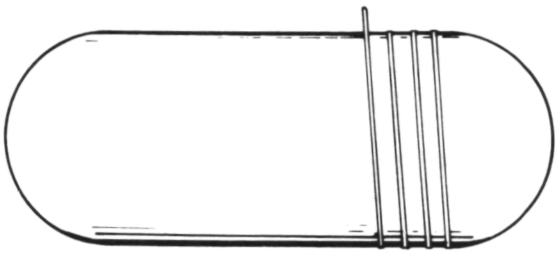

Hoop Winding Pattern

Tanks used for transportation and storage of gases are usually constructed from thick and heavy metal cylinders that are designed to prevent possible explosion. Because of their weight, they are difficult to handle and transport. Yet, if tanks are made lighter, their safety characteristics may be jeopardized.

Lightweight oxygen tanks have been produced by wrapping stainless steel liners with fiberglass filament. The resulting structure exhibits the strength characteristics of much heavier metal cylinders.

In this process thin stainless steel tank liners (see figure) are wrapped entirely with fiberglass filament in a longitudinal geodesic pattern that is alternated with hoop layers. The patterns cover the entire tank surface and are wound with uniform fiberglass thickness to provide uniform stress over the entire cylinder area.

The process is accomplished by internal pressurization of the liner to assure sufficient rigidity. The liner is then installed on the wind axis adapter which is part of the winding apparatus. The apparatus uses fully-adjustable longitudinal and circular arms designed for precise winding of polar and hoop layers of fiberglass at prescribed angles, tensions, and locations. Both arms supply pretensioned S-glass strands (magnesium-aluminum silicate composite) collected from the spools.

Fiberglass is wound in three winding and cure sequences, with the first two followed by grit blasting of the surface before the final step. The angles of winding are very important in this technique. They have been evaluated by a computer program and are dependent on the desired design characteristics. The result is a uniformly stressed metal liner assembly with excellent structural characteristics.

Source: J. F. Shuessler and R. J. Dannenmueller of McDonnell Douglas Corp. under contract to Marshall Space Flight Center (MFS-22470)

Circle 20 on Reader Service Card.

BEAM LEAD FORMING TOOL

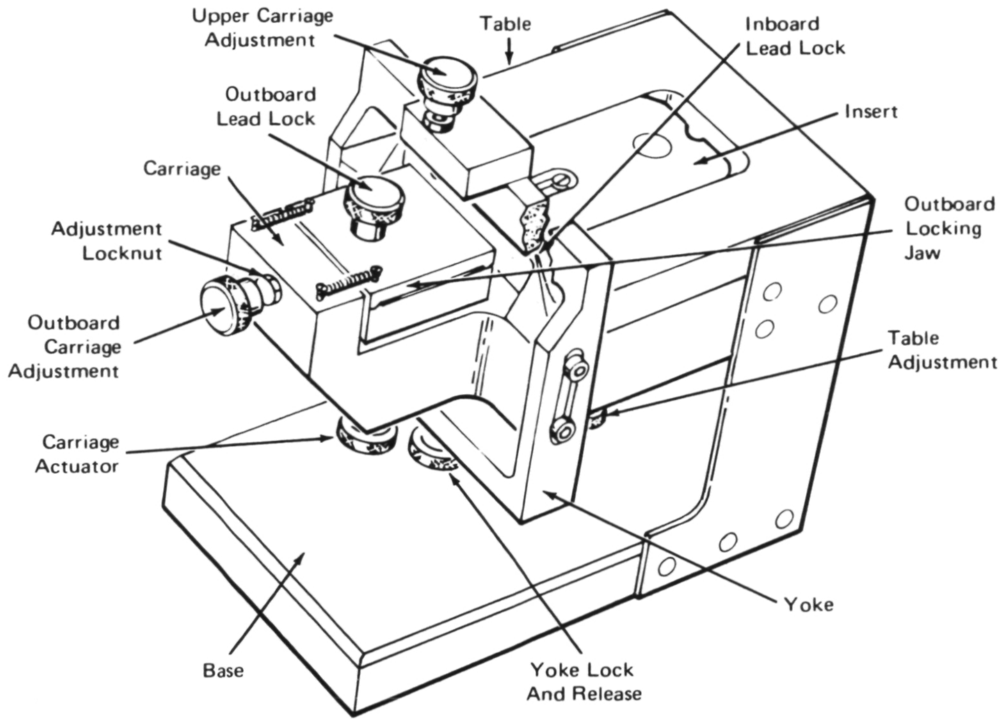

Manufacturers of flat-pack electronic devices, such as integrated circuit packages, have a variety of tools for bending the beam leads. Most of these tools, however, are designed for bending the leads to a fixed angle.

A tool was designed for table-top manual operation that can bend leads to any desired angle up to 90°. It can be readily adapted to electrical, hydraulic, or pneumatic operation.

The tool can handle lead lengths to 1/4 inch (0.6 cm). The desired angle of the lead is formed by positioning the flat pack on the tool table (see figure), and the table is adjusted vertically to aline the lower side of the lead with the inboard leak lock of the yoke. The lead is then inserted and locked between the jaws of the yoke. The carriage is then adjusted to a specified length required for the bend. The adjusting screws and the insert are preset to the required position dictated by the bend of the leads, and the outboard locking jaw of the carriage is locked on the other end of the lead. The carriage is then moved upward by means of a carriage actuator until it has reached the upper adjustment screw which stops the carriage at the preset bend angle. As the final step of the operation, the yoke lock is released and adjusted vertically to clear the bend lead, the outboard locking jaw is released, and the flat pack removed from the device.

Source: P. W. Clemons of
Sperry Rand Corp.
under contract to
Marshall Space Flight Center
(MFS-22133)

Circle 21 on Reader Service Card.

COMPATIBILITY OF MATERIALS WITH LIQUID OXYGEN

The impact sensitivity of materials in the presence of liquid oxygen has been determined for a large number of commercially available materials, and the results have been published in a report. Over 2,000 different materials have been subjected to a total of 240,000 tests.

The data have been compiled and tabulated, and recommendations are made for the selection of safe materials for use in oxygen environments. The materials discussed fall into the following categories:

Lubricants
Sealants and Threading Compounds
Thermal and Electrical Insulation
Elastomers, Plastics, and Adhesives
Gaskets and Packing Materials
Metals, Alloys, and Solders
Solvents, Cleaning Solutions, and Miscellaneous Chemicals
Dye Penetrants

The tests were made with a modified Impact Sensitivity Tester and consisted of dropping a plummet, of known weight from a known distance, on a striker pin. The striker pin rests on the test material which is in a cup of liquid oxygen. The material is first tested with a drop height of over one meter. If the test material is oxygen sensitive, it will explode or flash brilliantly. Tests are then made at regularly reduced heights until no reaction occurs.

Each material is given two ratings, one for the particular sample or lot tested and one for the material in general. Ratings assigned include satisfactory, satisfactory if each purchased sample is tested, satisfactory if each manufactured batch is tested, and unsatisfactory. It should be noted that materials which are basically compatible with liquid oxygen can be rendered potentially hazardous by traces of impurities.

Source: C. F. Key
Marshall Space Flight Center
(MFS-22872)

Circle 22 on Reader Service Card.

ADHESIVE BONDING OF HYBRID MICROCIRCUITS

Adhesive bonding is one of the better methods of assembling hybrid microcircuits. A set of guidelines for the selection of adhesives helps designers choose those that will meet the long-life, high-reliability requirements of modern electronic equipment. A study has been made to identify the properties of electrically insulative adhesives that could potentially cause failure, and evaluation tests have been developed to quantify these properties. This study is the basis for the guidelines and specifications. Bond strength, outgassing after cure, and corrosion susceptibility are studied in detail, since these properties are especially critical.

The guidelines include a tabulation and discussion of the most commonly used adhesives. This includes a general review of polymeric adhesives, and identification of the major types of adhesives commercially available and specifically designed for microelectronic use. Comparative results are given for selected adhesives.

Source: S. V. Caruso
Marshall Space Flight Center and
K. L. Perkins and J. J. Licari of
Rockwell International Corp.
under contract to
Marshall Space Flight Center
(MFS-22908)

Circle 23 on Reader Service Card.

DESIGN AND MATERIAL SELECTION FOR INVERTER TRANSFORMER CORES

Power supplies often incorporate an inverter to obtain high voltage from low-voltage power sources. Typically, dc power from a low-voltage source is fed to the primary of a step-up transformer by a pair of power transistors which are alternately switched on and off by an oscillator drive. The square-wave output of the secondary is subsequently rectified and filtered. Because of the inductive nature of the transformer, excessive voltage spikes often appear if the transformer saturates, and when spikes exceed the ratings of the transistors connected to the inverter, there is high probability of system failure.

It is desirable to minimize voltage spikes by proper construction of transformers, but the design of reliable, efficient, and lightweight transformers for inverters has been hampered seriously by the lack of engineering data describing the behavior of core materials operating at 2400-Hz square-wave excitation.

A report is now available which describes in detail the results of a program of investigation undertaken to study the magnetic properties of candidate materials for use in spacecraft transformers, static inverters, converters, and transformer-rectifier power supplies; but the information is also applicable to the design of transformers for nonaerospace use. The report includes many illustrations of B-H loop patterns and the output waveforms obtained with various materials in a typical inverter system. Operational parameters are discussed, especially with reference to core saturation and air gap.

The report summarizes the results of a series of tests performed on commercially available magnetic alloys to determine their dc and ac characteristics at 2400-Hz square-wave excitation. The tests were performed on cut and uncut cores (in both toroidal and C forms) for comparison of gapped and ungapped core magnetic properties. The test apparatus consisted of a power oscillator to drive the test transformer (1:1) and a current probe to indicate current waveforms in the primary. The secondary of the transformer was loaded by a suitable resistor in series with a switch and a diode; with the switch closed, secondary current was rectified by the diode to produce a dc bias in the secondary winding.

For the investigation of core saturation, cores were fabricated in a basic configuration for toroidal cores. The test transformer consisted of 54-turn primary and secondary windings, with square-wave excitation on the primary. For the investigation of air gap effects, both toroidal and C-types of core configurations were tested in the gapped and ungapped states. As fabricated conventionally, toroidal cores are virtually gapless; to increase the gap, cores were cut in half and the edges were lapped, etched with acid to remove cutting debris, and banded to form the core.

The report includes material characteristics for available alloy compositions in tabular form, including: trade names, saturated flux density, dc coercive force, loop squareness, material density, and watts per pound at 3 kHz.

Source: William T. McLyman of
Caltech/JPL
under contract to
NASA Pasadena Office
(NPO-11726)

Circle 24 on Reader Service Card.

STRESS-CORROSION CRACKING SUSCEPTIBILITY OF 18Ni MARAGING STEEL

A series of age-hardenable high-nickel martensitic steels, called maraging steels, have yield strengths ranging from 1.379×10^6 N/m^2 (200 ksi) to 2.413×10^6 (350 ksi). The desired strength can be obtained by a simple aging process (3 hours at 750 K or 900° F) and the steel is classified according to yield strength (grades 200 to 350). Because of their strength, ductility, fabricability, and fracture toughness, 18-percent nickel (18Ni) maraging steels are used in aerospace hardware, pressure vessels, railroad equipment, and the petrochemical industry.

Although maraging steels are more resistant to rusting than most of the non-corrosion-resistant steels, some type of protective coating is normally used for prolonged service. These steels also are known to be susceptible to stress-corrosion cracking (SCC). An investigation has been made to determine the degree of this susceptibility.

The resistance of several grades of 18Ni maraging steel is determined in 3.5 percent salt (NaCl) solution, synthetic sea water, high humidity, and outside atmosphere. Four types of specimens were used to test SCC resistance in at least two directions of grain orientation. Flat tensile specimens were used for testing sheet material and were beam loaded by constant deflection. Round tensile specimens, stressed in uniaxial tension, were used for testing the longitudinal and long transverse grain directions of plate and the longitudinal grain direction of bar stock. The transverse grain direction of bar stock was evaluated using C-rings loaded by constant deflection. Compact tension specimens, dead-weight loaded in the transverse grain direction, were used in the fracture mechanics approach. Specimens were deflected or strained to the desired stress levels (40 to 90 percent of the directional yield strength), as calculated from measured mechanical properties.

All grades of the maraging steel were found to be susceptible to SCC in varying degrees according to their strengths, with the lowest strength steel being the least susceptible and the highest strength steel the most susceptible.

The SCC resistance of 250 grade maraging steel is evaluated in salt and salt-chromate solutions using fracture mechanics techniques. The threshold value is approximately 4.4×10^4 $(N/m^2)\sqrt{m}$ [40 (ksi)$\sqrt{in.}$].

Source: T. S. Humphries and E. E. Nelson
Marshall Space Flight Center
(MFS-23044)

Circle 25 on Reader Service Card.

Patent Information

The following innovations, described in this Compilation, have been patented or are being considered for patent action as indicated below:

Fatigue Testing Device (Page 4) LAR-10426

This invention is owned by NASA (U. S. Patent No. 3,795,134). Inquiries concerning nonexclusive or exclusive license for its commercial development should be made to:

Patent Counsel
Langley Research Center
Mail Stop 313
Hampton, Virginia 23665

Beam Lead Forming Tool (Page 22) MFS-22133

Inquiries concerning rights for the commercial use of this invention should be addressed to:

Patent Counsel
Marshall Space Flight Center
Code CC01
Marshall Space Flight Center, Alabama 35812

U.S. Government Printing Office: 1976-638-230 Region 3-II

"The aeronautical and space activities of the United States shall be conducted so as to contribute . . . to the expansion of human knowledge of phenomena in the atmosphere and space. The Administration shall provide for the widest practicable and appropriate dissemination of information concerning its activities and the results thereof."

—NATIONAL AERONAUTICS AND SPACE ACT OF 1958

NASA TECHNOLOGY UTILIZATION PUBLICATIONS

These describe science or technology derived from NASA's activities that may be of particular interest in commercial and other non-aerospace applications. Publications include:

TECH BRIEFS: Single-page descriptions of individual innovations, devices, methods, or concepts.

TECHNOLOGY SURVEYS: Selected surveys of NASA contributions to entire areas of technology.

OTHER TU PUBLICATIONS: These include handbooks, reports, notes, conference proceedings, special studies, and selected bibliographies.

Details on the availability of these publications may be obtained from:

National Aeronautics and
Space Administration
Code KT
Washington, D.C. 20546

Technology Utilization publications are part of NASA's formal series of scientific and technical publications. Others include Technical Reports, Technical Notes, Technical Memorandums, Contractor Reports, Technical Translations, and Special Publications.

Details on their availability may be obtained from:

National Aeronautics and
Space Administration
Code KS
Washington, D.C. 20546

NATIONAL AERONAUTICS AND SPACE ADMINISTRATION
Washington, D.C. 20546